Brain Stimulation 15 (2022) 769–779

Contents lists available at ScienceDirect

Brain Stimulation

journal homepage: http://www.journals.elsevier.com/brain-stimulation

Mechanistic insights into ultrasonic neurostimulation of disconnected neurons using single short pulses☆

Eyal Weinreb *, Elisha Moses

Department of Physics of Complex Systems, Weizmann Institute of Science, Rehovot, 7610001, Israel

ARTICLE INFO

Article history:
Received 11 October 2021
Received in revised form
27 April 2022
Accepted 3 May 2022
Available online 11 May 2022

Keywords:
Ultrasonic neuromodulation (UNMOD)
Focused ultrasound neuromodulation (FUN)
Transcranial ultrasound stimulation (TUS)
Transcranial focused ultrasound (tFUS)
Transcranial pulsed ultrasound (tPUS)
Low-intensity focused ultrasound (LIFUS)

ABSTRACT

Ultrasonic neurostimulation is a potentially potent noninvasive therapy, whose mechanism has yet to be elucidated. We designed a system capable of applying ultrasound with minimal reflections to neuronal cultures. Synaptic transmission was pharmacologically controlled, eliminating network effects, enabling examination of single-cell processes. Short single pulses of low-intensity ultrasound were applied, and time-locked responses were examined using calcium imaging.

Low-pressure (0.35 MPa) ultrasound directly stimulated ~20% of pharmacologically disconnected neurons, regardless of membrane poration. Stimulation was resistant to the blockade of several purinergic receptor and mechanosensitive ion channel types. Stimulation was blocked, however, by suppression of action potentials. Surprisingly, even extremely short (4 μs) pulses were effective, stimulating ~8% of the neurons. Lower-pressure pulses (0.35 MPa) were less effective than higher-pressure ones (0.65 MPa). Attrition effects dominated, with no indication of compromised viability.

Our results detract from theories implicating cavitation, heating, non-transient membrane pores >1.5 nm, pre-synaptic release, or gradual effects. They implicate a post-synaptic mechanism upstream of the action potential, and narrow down the list of possible targets involved.

1. Introduction

A major issue hindering the advancement of US neurostimulation is the lack of a concrete understanding of the underlying mechanism through which acoustic pressure stimulates neuronal activity. Several possible mechanisms have been proposed, but as yet, none are widely accepted in the field. Mechanisms discussed [1–4] include sonoporation [5], membrane distortion [6] and temperature increases [7–16], as well as synaptic vesicle fusion [17,18] and direct effects on ion channels [5,19–24].

Several experimental issues can confound mechanistic study of US neurostimulation. First, acoustic reflections can distort the spatial and temporal characteristics of the applied US pressure [25–28]. While these reflections can be modeled and accounted for using computational methods that will be critical for the translational applications of US [26,29–33], these reflections make quantitative studies more complex, and demand higher accuracy in the experimental system. Second, when stimulating highly connected neuronal networks, recurrent activity can obscure single-cell level mechanisms, and observed responses may reflect downstream effects of processes occurring outside the examined area. Third, US pulse trains can contain confounding envelope frequencies that emerge from the initiation and termination of individual pulses [34].

We present an experimental system that addresses these issues, enabling the examination of processes governing US stimulation at the single-neuron level. We applied single US pulses to neuronal cultures with minimal acoustic reflections. Synaptic transmission was pharmacologically blocked, eliminating network effects. Optical methods were used to measure neuronal activity and integrity

Abbreviations: AP, Action Potential; APV, 2-Amino 5-Phosphonopentanoic Acid; CNQX, Cyanquixaline; CNS, Central Nervous System; FOV, Field of View; GABA, Gamma-Aminobutyric Acid; IACUC, Institutional Animal Care and Use Committee; IC_{50}, Half Maximal Inhibitory Concentration; IQR, Interquartile Range; MS, Mechanosensitive; NBLS, Neuronal Bilayer Sonophore; NMDA, N-Methyl-D-Aspartic Acid; Na_V, Voltage Gated Sodium; PCD, Passive Cavitation Detection; PI, Propidium Iodide; ROI, Region of Interest; RR, Ruthenium Red; SEM, Standard Error of the Mean; TLC, Thermochromic Liquid Crystal; TTX, Tetrodotoxin; UB, Unstimulated Baseline Activity; US, Ultrasound.

☆ Part of this work was previously presented at the 3rd International Brain Stimulation Conference.

* Corresponding author.
E-mail addresses: eyal.weinreb.u@gmail.com (E. Weinreb), elisha.moses@weizmann.ac.il (E. Moses).

https://doi.org/10.1016/j.brs.2022.05.004

under the application of US, while pharmacological interventions disrupted specific cellular processes, allowing the examination of each process' role in the mechanism of US neurostimulation.

We used this system to examine and rule out many of the proposed mechanisms, as well as eliminate the candidacy of several ion channels and receptors as the main players in US stimulation. We report a surprising observation of effective stimulation using single extremely short pulses. We also observed significant attrition effects, who's source has yet to be identified.

2. Methods

2.1. Neuronal cultures

This study was approved by the Weizmann IACUC.

We used dissociated rat hippocampal neural cultures grown on circular glass coverslips [35,36]. These cultures develop into flat, interconnected networks containing 70%–80% excitatory and 30%–20% inhibitory neurons [37]. Neuronal activity was monitored via calcium imaging. This allowed measurement of hundreds of neurons simultaneously while affording easy pharmacological intervention.

Neuronal connectivity was disconnected using a cocktail of synaptic transmission blockers consisting of bicuculline ($GABA_A$ inhibitory receptor antagonist) with CNQX and APV (non-NMDA and NMDA excitatory glutamate receptor antagonists respectively).

In the disconnected cultures, we used TTX to block Na_V channels, eliminating neuronal APs; PI to image membrane poration; RR and GsMTx-4 to block MS ion channels; and suramin to block P2 purinergic receptors.

These methods are detailed in the supplementary.

2.2. Experimental system

The system consisted of a US transducer in a water chamber mounted onto an inverted fluorescence microscope. Cultures were positioned at the convergence of the acoustic and optic focus, enabling imaging of the cultures while simultaneously exposing them to US (Fig. 1A).

US reflections were minimized by optimizing acoustic impedance matching, having minimal obstructions in the acoustic path, and absorbing the residual acoustic energy.

A 2D large-scale simulation of the basic chamber architecture (Fig. 1B) shows that the interaction of US with the air chamber that houses the objective doesn't disrupt the homogeneity or location of the US focus. A 3D high-resolution simulation near the culture glass (Fig. 1C) shows that the US pressure is mostly constant over the entire FOV, and reflections from the thin coverslip glass are minimal.

The low level of reflections in the system was verified using a hydrophone in the experimental chamber (see supplementary text and Fig. S4). The location and size of the US focus were examined using a TLC sheet (Supplementary Fig. S5).

We used single pulses, a fundamental frequency of 500 kHz, peak pressures of 0.35–1.32 MPa, and durations of 4 μs-40 ms. The parameters for each experiment are detailed in the supplementary.

The pressure output of the transducer, as well as the duration of the extremely short pulses were verified using a hydrophone in a large water tank.

The design, simulation, and verifications of the system are detailed in the supplementary.

2.3. Experimental procedure

Cultures were placed into the experimental chamber, and their spontaneous activity was first imaged to verify vitality and identify active cells. Pharmacological agents were then introduced and allowed 10 min to take effect.

For each stimulation, cultures were exposed to a single US pulse, and time-locked images were acquired for 5 s before and 10 s after.

Calcium imaging was done using Fluo-4. Such chemical calcium indicators can compromise the culture's vitality over time, so cultures were imaged for a few hours and then disposed of. Alternatively, where stated, the genetically encoded indicator GCaMP was used, and measurements were conducted over a longer period, and over multiple experimental sessions.

The experimental procedure is detailed in the supplementary.

2.4. Analysis

In experiments involving intact networks, the mean fluorescent intensity for the entire FOV was taken.

In experiments involving disconnected networks, ROIs were automatically defined over active cell bodies. Automated response detection was then performed for each ROI by examining changes in its intensity following the stimulation. The unstimulated baseline activity was characterized by examining changes in the intensity *before* the stimulation. Comparison of the evoked activity to this unstimulated baseline aided in the differentiation of the evoked activity from any spontaneous activity that remained after network disconnection and from noise-related false detections.

These methods are detailed in the supplementary, along with the calculation of a response's amplitude, duration, and latency. Statistical tests and figure methods are also detailed in the supplementary.

Spontaneous network activity was evaluated before disconnection and the number of neurons that participated in a burst were counted. The number of these "generally active" neurons was used to normalize the number of neurons that respond after disconnection. There were typically ~200 generally active cells within the FOV (191.4 ± 10.2, mean ± SEM, $n^c = 78$).

Throughout this paper n^c refers to the number of cultures included in the analyses, n^s to the number of stimulations, and n^n to the number of cells.

3. Results and discussion

3.1. Single US pulses stimulated fully connected neuronal cultures

US reproducibly generated robust group calcium responses immediately following stimulation. Fig. 2A shows example stimulations of a fully connected culture.

These cultures naturally display spontaneous bursts of all-or-none synchronous activity, stemming from their extensive connectivity [38]. The evoked responses were consistent in amplitude and shape over time and similar to spontaneous bursts. Spontaneous activity continued even after multiple stimulations, and stimulations given during a previously occurring spontaneous burst didn't initiate additional bursts, as is demonstrated by the fifth burst in the example in Fig. 2A. This all hints at a non-destructive stimulation mechanism involving physiological neuronal activation processes.

The pressure levels (0.67 MPa) at the frequency used are too low to cause cavitation [39] or significant thermal effects, detracting from these mechanisms, which is encouraging for safe use in humans. To further rule out the possibility of cavitation, we present Supplementary Fig. S7, in which passive cavitation detection (PCD)

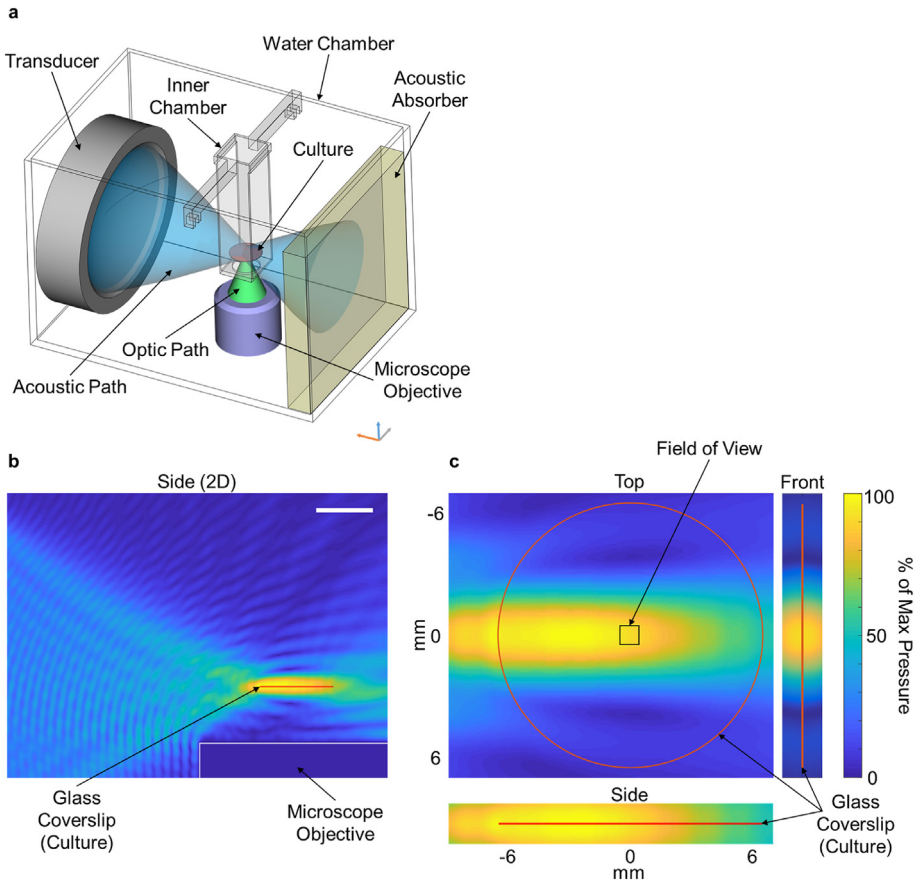

Fig. 1. Experimental chamber
A: The US transducer was mounted in a water chamber on an inverted microscope. The culture was positioned at both the acoustic and optic focus within an inner chamber filled with imaging medium. US passed from the transducer, through a mylar sheet into the inner chamber, through the culture, through a second mylar sheet back out into the water chamber, and into an acoustic absorber. US was applied to the culture from the side, at a 90° angle to the optic axis, keeping the objective out of the acoustic path, preventing reflections. Cross scale: 10 mm. **B:** 2D large-scale simulation of the basic chamber architecture. Culture glass is shown as a guide, and is not part of the 2D large-scale simulation. Spatial resolution of simulation grid: 500 μm. Scale bar: 10 mm. **C:** 3D high-resolution simulation of the acoustic pressure being applied to the culture glass. Image slices of the 3D volume are located at the center of the culture glass. Spatial resolution of simulation grid: 50 μm.

[40] indicates that cavitation is not a factor at the pressures and durations of the pulses we use.

This is in line with several other studies that have reported successful stimulation of in-vitro CNS neurons [14,17,20,23,41–50].

3.2. Single US pulses stimulated pharmacologically disconnected neurons

We disconnected the neurons by pharmacologically blocking synaptic transmission, enabling examination of mechanisms at the single-cell level without population effects, and separating post-synaptic processes from those upstream. When disconnected, spontaneous activity shifts from all-or-none bursts to sporadic, uncorrelated single-neuron events [51].

Single US pulses successfully generated calcium responses in disconnected cultures. As shown in Fig. 2B (blue), ~20% of the generally active cells were stimulated by US after disconnection.

This shows that US can generate supra-threshold neuronal excitation without requiring network amplification. Stimulation of neurons with blocked synaptic inputs indicates that US has a direct effect downstream of the synaptic transmission, and is not just causing pre-synaptic neurotransmitter release.

This is in line with Tyler et al. (2008) [17], who showed that US stimulation, measured as vesicle exocytosis, was resistant to blockade of excitatory input. They also showed that disruption of the neuronal machinery for vesicle release eliminated this effect, indicating that US didn't directly cause vesicle membrane fusion.

Recent in-vitro studies paint a more complex picture of the necessity of a pre-synaptic mechanism. Some showed, in line with our observations, that blockade of excitatory connectivity didn't completely eliminate US stimulation, while others reported that it did [20,50,52]. Interestingly, those experiments that agreed with ours both used calcium imaging, as we did, while those that disagreed both used multielectrode arrays.

One hypothesis as to why only a subset of neurons are responsive to stimulation is that the neurons differ in their excitation thresholds. This could be similar to what we have previously reported with electrical stimulation [53], where the orientation of the neuronal processes with regard to the vector of the applied electric field affects the neuron's sensitivity. Another possibility is the differential expression of certain MS channels in distinct neuronal cell types [54]. Neuronal cell types also differ in their morphology which can affect the overall mechanical properties of their membrane [55].

External activation of bursts in connected cultures requires the initial stimulation of only a small fraction of neurons (3–5%) [51], so these 20% are more than enough to generate the stimulation we observed in connected networks. Nevertheless, it is still possible that additional neurons were directly activated in the connected

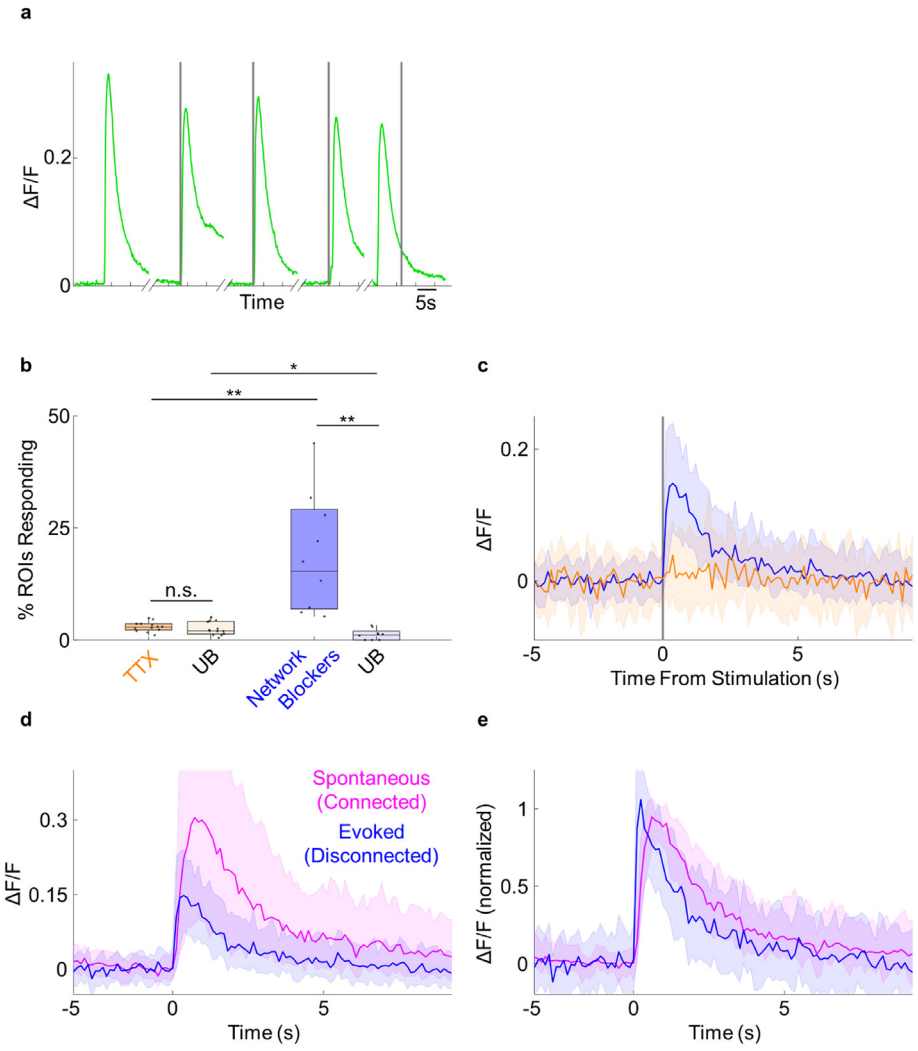

Fig. 2. Stimulation of connected and disconnected cultures
A: Example stimulation of a connected culture. Mean calcium traces from the entire FOV. Shown is an unstimulated spontaneous burst, three successful stimulations, and an unsuccessful stimulation applied during a previous spontaneous burst. **B:** Percentage of generally active cells responsive to stimulation in disconnected cultures. ~20% (19.4 ± 4.4%, UB = 1.3 ± 0.4%, $n^{s,c}$ = 9, blue) of the cells responded to US. With additional TTX the efficacy was much smaller and similar to the unstimulated baseline activity (3 ± 0.3%, UB = 2.5 ± 0.4%, $n^{s,c}$ = 13, orange). (mean ± SEM, UB - unstimulated baseline activity) **C:** Median calcium traces from the responsive cells, corresponding to **B**. n^{n}(blue) = 179, n^{n}(orange) = 65. **D:** Median calcium traces of an evoked response after disconnection (blue) and of a spontaneous burst prior to disconnection (magenta), in the same responsive cells. n^{n} = 179. **E:** Same as **D**, each trace normalized by its peak intensity (before averaging). In this, and in all following figures unless indicated otherwise - Boxplot lines mark the median, boxes extend 25th-75th percentiles, whiskers extend to the most extreme data that are within 1.5 × IQR from the box. In traces, 25th-75th percentiles are shown shaded, vertical gray line marks the time of stimulation. *p < 0.05; **p < 0.01; ***p < 0.001; p > 0.05, not significant (n.s.). (For interpretation of the references to colour in this figure legend, the reader is referred to the Web version of this article.)

culture and that some part of that response *was* eliminated by blocking the synapses.

Fig. 2D and E show the evoked response after disconnection (blue) and the spontaneous burst prior to disconnection (magenta), in the same responsive cells. Although the overall response dynamics were similar, the evoked response had a lower amplitude (0.19 ± 0.02 vs. 0.61 ± 0.06 ΔF/F) and a shorter duration (1.01 ± 0.05 vs. 1.91 ± 0.08 s) (mean ± SEM, p < 0.001, n^{n} = 179). 28 ± 7.8% of the US responsive cells were not considered responsive during the spontaneous burst. The shorter duration and lower amplitude make sense, as the neurons in the disconnected network are expected to have fewer APs than in the connected network, due to lack of feedback excitation loops.

To get a sense of scale for the response amplitude, electrical stimulation of a disconnected culture generated an amplitude of 0.04 ± 0.002 ΔF/F (mean ± SEM, n^{n} = 131), although this is reported to strongly depend on the stimulation and imaging parameters [53].

The observed spatial distribution was not significantly different between the responsive cells after network disconnection and the generally active cells prior to disconnection. This was measured by the mean distance of the cells (within the 0.9 mm^2 FOV) from their centroid: (312 ± 26 μm for responsive cells vs. 337 ± 11 μm for generally active cells, mean ± SEM, p = 0.20, $n^{s,c}$ = 9). This confirms that the focal area of effective stimulation covered the entire FOV.

3.3. AP blockade abolished the response to US

We used TTX to block Na_V channels, eliminating neuronal APs, separating postsynaptic processes from those downstream.

Fig. 2B (orange) shows the efficacy of US, after network disconnection and additional AP blockade. AP disruption

eliminated the response to US. This indicates that the mechanism being affected by US is upstream of the AP or is the AP process itself. It's not a lasting poration of the plasma membrane, nor is it a large calcium influx or intracellular calcium release directly generated by US, as these processes would not depend on functioning APs.

This is in line with Tyler et al. (2008) [17], showing AP disruption eliminates the response to US in hippocampal slices. This was also shown in connected networks [41,43,50].

3.4. US stimulation was not associated with membrane poration

A membrane integrity assay using PI showed that only a small percentage (4.6 ± 1%, mean ± SEM, $n^{s,c} = 5$) of successfully stimulated disconnected cells became permeable during stimulation. An example is shown in Fig. 3.

This confirms that long-term poration is not part of the stimulation process. Pores that are very transient, or smaller than the 1.5 nm detection level of PI [56], may still be relevant [57].

3.5. Extremely short US pulses stimulated disconnected neurons

Several proposed mechanisms of US neurostimulation rely at low intensities on a gradual accumulation of effects. To exclude such mechanisms, we used extremely short pulses of only a 2-cycle duration, corresponding to 4 μs at 500 kHz, 10,000 times shorter than the 40 ms pulses common in the literature.

Fig. 4A shows the efficacy of 40 ms and 4 μs duration pulses, after network disconnection. A clear response even to the extremely short pulses is evident.

This is a surprising result. It points at molecular scale processes, which could occur at these time scales. It precludes mechanisms such as stable cavitation, which can generate strong forces through energy accumulation [58], but would necessitate longer pulses. We calculate heating with our pulse parameters at ~5×10^{-5} °C/ms which would also require longer pulses to matter.

This is encouraging from a translational standpoint, as extremely short pulses are much safer than longer ones [59], with intensities far below many regulatory limits [60]. They also allow more intricate spatiotemporal patterning and are less prone to form standing waves. While previous studies have used shorter pulses as part of long pulse trains, the shortest single pulses shown to stimulate unmodified neurons were 100 μs long [46], an order of magnitude longer than ours. This remarkable result warrants extensive further investigation.

Standard duration pulses activated more cells than the extremely short ones. This is in line with a recent in-vitro study showing lower stimulation thresholds for longer pulses [25].

Longer pulses may simply recruit additional cells as the pulse goes on. To test this, we imaged the initial response dynamics at a high sampling rate (~1 kHz). At this rate technical camera limitations constrain imaging to the averaged response over the entire FOV, including many cells. Fig. 4C and D show an observable difference in the initial dynamics of the responses, with a longer latency in response to the longer pulse than to the shorter one (27.5 ± 3.1 ms, $n^s = 6$ vs. 16.8 ± 1.5 ms, $n^s = 7$; $n^c = 4$; mean ± SEM; $p < 0.05$), indicating that the longer pulse doesn't simply accumulate responsive cells, rather that the two pulse durations have different effects. There may be an ongoing interaction of the pulse with the neuronal physiology, disrupting the initiation of the response. Alternatively, different pulse durations may be exciting different types of neurons with distinct inherent dynamics.

The NBLS model [6] suggests that during the pulse there is an accumulation of charge, due to changes in the membrane's capacitance, which gradually depolarizes the neuron with each cycle. This mechanism is therefore strongly dependent on pulse duration. We implemented the model using Matlab, and it projected generation of APs only for pulses longer than 5 ms (for a pressure peak of 0.5 MPa). Thus, it is at odds with our observation. Fig. 4F shows the model's projected membrane potential during stimulation both with an extremely short pulse and with a standard duration one.

3.6. P2 receptor blockade did not eliminate the response to US, efficacy increased with pressure

P2 purinergic receptors play a crucial role in MS processes [61], and may be relevant for US stimulation. Fig. 5A shows the efficacy of pulses at peak pressures of 0.35 MPa and of 0.67 MPa, after disconnection and additional blockade of P2 receptors using suramin.

Blocking P2 receptors did not prevent stimulation. Thus, purinergic signaling is not a necessary part of the mechanism. It should be noted that suramin (in reference to $P2Y_2$ receptors) was used at a moderate concentration of twice the IC_{50}. Suramin is neurotoxic above this concentration [62].

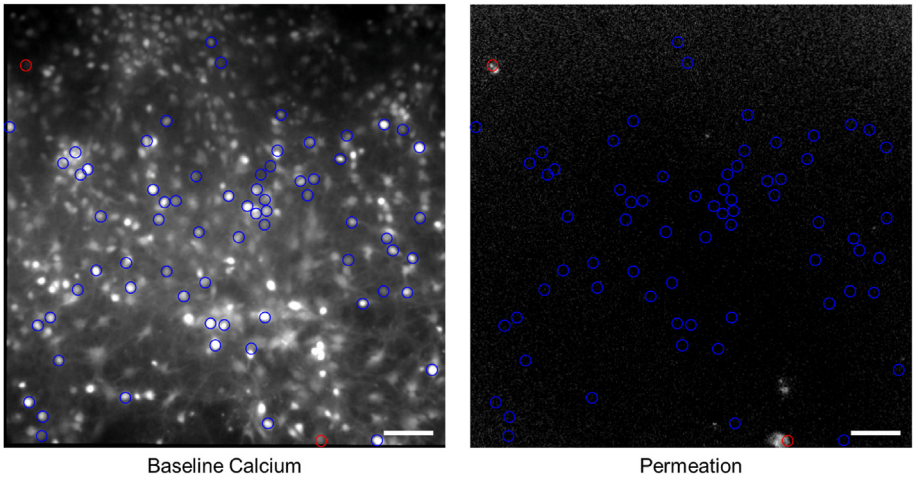

Fig. 3. Example of membrane integrity assay using PI
A single stimulation in a disconnected culture. 68 of the generally active cells responded (blue), only 2 of them had become permeable during stimulation (red). **Left:** Calcium imaging baseline before stimulation. **Right:** PI fluorescence imaging. Intensity increase from before stimulation to 10 min after. Scale bar: 100 um. (For interpretation of the references to colour in this figure legend, the reader is referred to the Web version of this article.)

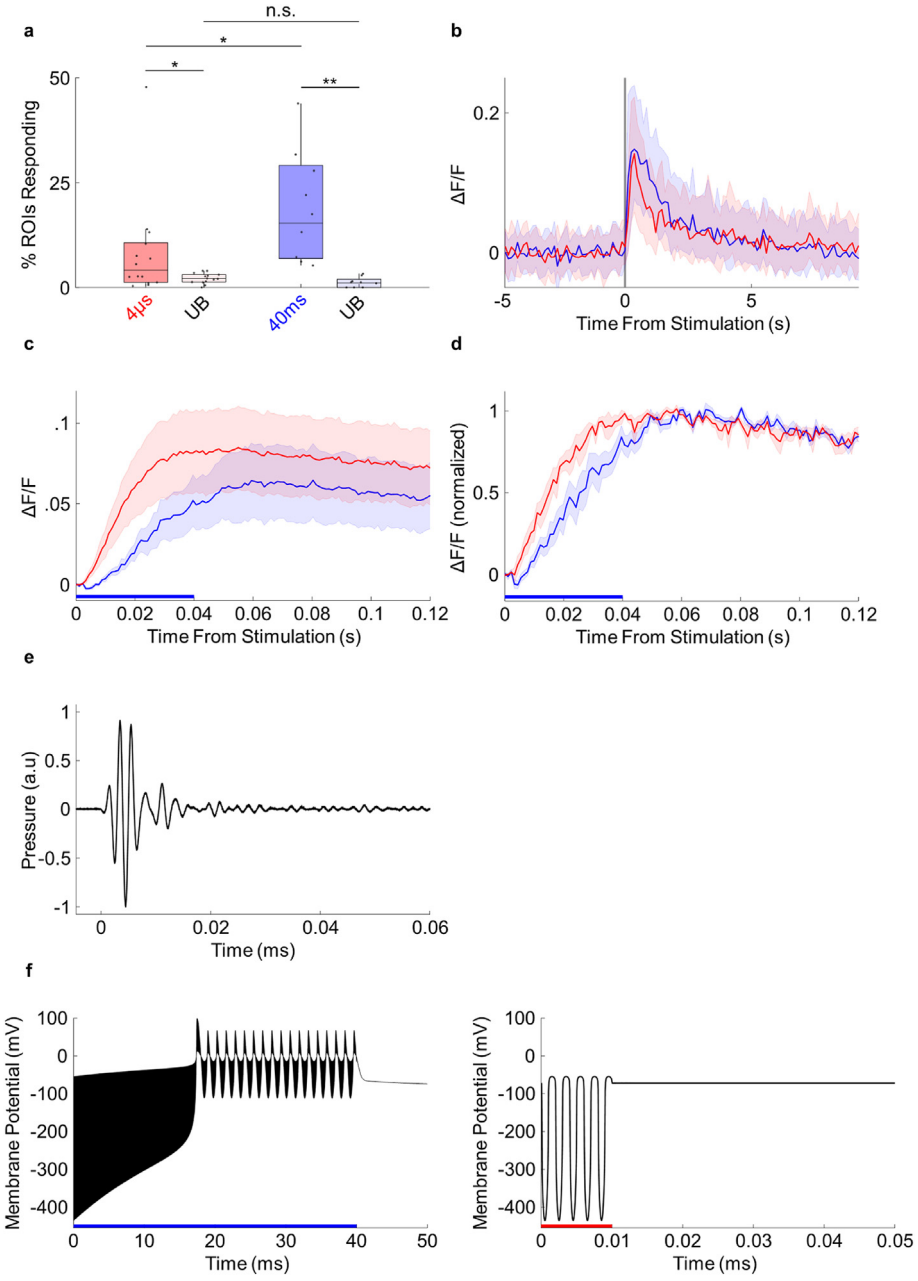

Fig. 4. Stimulation with extremely short pulses

A: Percentage of generally active cells responsive to short 4 μs (8.3 ± 3.3%, UB = 2.2 ± 0.3%, $n^{s,c} = 14$, red), and to standard 40 ms (19.4 ± 4.4%, UB = 1.3 ± 0.4%, $n^{s,c} = 9$, blue) pulses, in disconnected cultures (mean ± SEM). Removal of the outlier in the short pulse group did not change this outcome. UB - unstimulated baseline activity. **B:** Median calcium traces from responsive cells, corresponding to **A**. n^n(red) = 164, n^n(blue) = 179. **C:** Mean, full FOV, calcium traces of the initial response dynamics, in responsive disconnected cultures, at a high sampling rate. SEM shown shaded. Blue bar along the x-axis shows the standard pulse duration, the bar for the short pulse is too short to be visible. n^s(red) = 7, n^s(blue) = 6.**D:** Same as **C**, each trace normalized by its peak intensity (before averaging). **E:** Hydrophone measurement of the 4 μs pulse. The hydrophone was positioned ~1 mm above the center of the face of the culture glass within the experimental chamber. **F:** Simulation of the response in the NBLS model. Membrane voltage calculated with a standard 40 ms pulse (left, blue bar) and a short 10 μs pulse (right, red bar) using a peak pressure of 0.5 MPa. Multiple APs occur with the standard duration pulse, but none with the short one. (For interpretation of the references to colour in this figure legend, the reader is referred to the Web version of this article.)

The higher pressure activated more cells than the lower pressure. It also generated a higher response amplitude (0.55 ± 0.05 ΔF/F, $n^n = 532$ vs. 0.32 ± 0.04 ΔF/F, $n^n = 88$; mean ± SEM; $p < 0.001$). The response is shown in Fig. 5B. A possible cause for the increased amplitude is that longer bursts of multiple APs are generated in the responsive neurons, but this has not been verified. These results align with previous in-vitro [25,43,45,48] and in-vivo studies [20,63–65] showing stimulation efficacy increases with pressure.

3.7. MS ion channel blockade did not affect the efficacy of US

Several MS ion channel types have been implicated in the literature, notably TRPA, TRPC, TRPV, K2P, and Piezo channels [20–24,66,67].

Of these, RR blocks the TRPA, TRPV, TREK-2, and Piezo channels [68–70]. Fig. 5C shows the efficacy after network disconnection, with and without additional MS channel blockade using RR. RR

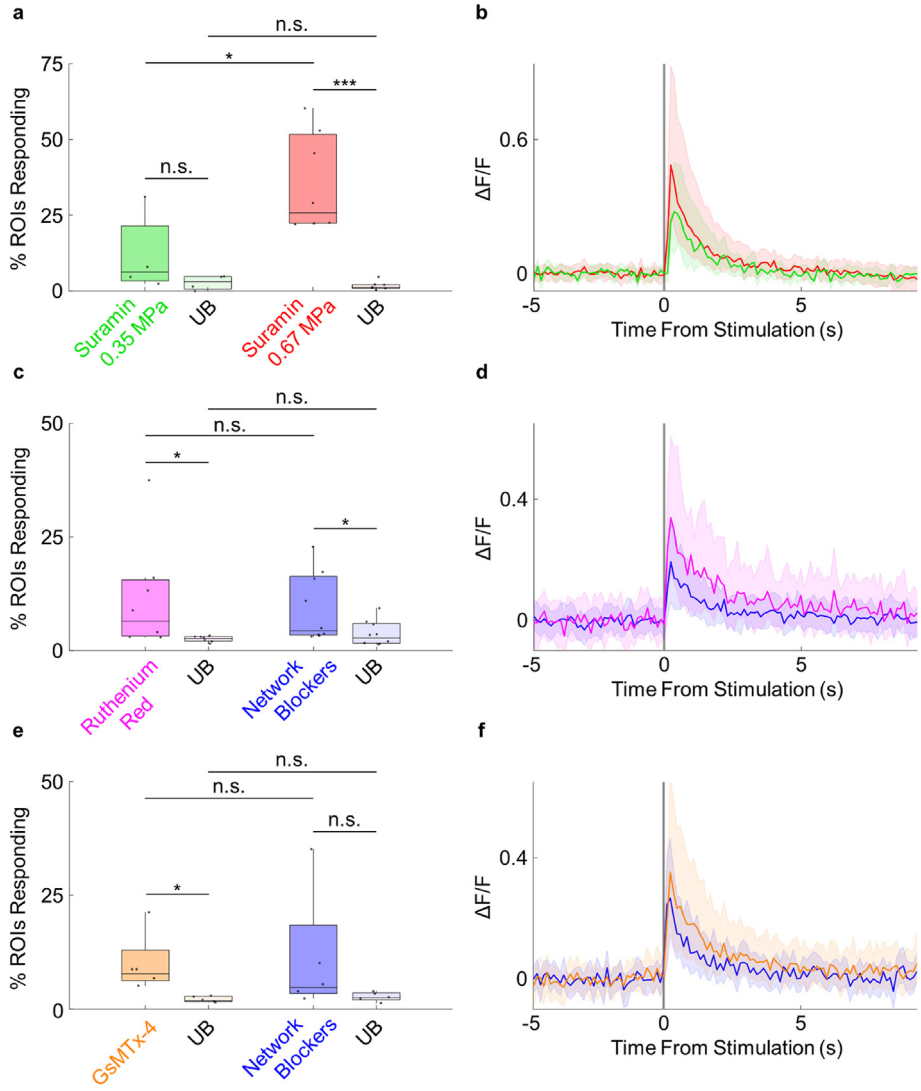

Fig. 5. Pharmacological blockade of MS ion channels and receptors
A, C, E: Percentage of generally active cells responsive to stimulation. UB - unstimulated baseline activity. **B, D, F:** Median calcium traces from responsive cells, corresponding to **A,C,E**. **A:** Suramin did not block the response in disconnected cultures. The higher pressure of 0.67 MPa was more effective (36.4 ± 6.1%, UB = 1.7 ± 0.5%, $n^{s,c} = 7$, red) than 0.35 MPa (11.5 ± 6.6%, UB = 2.7 ± 1.2%, $n^{s,c} = 4$, green) (mean ± SEM). **B:** n^{n}(green) = 88, n^{n}(red) = 532. **C:** The efficacy in disconnected cultures with additional RR (12.3 ± 4.6%, UB = 2.6 ± 0.3%, $n^{s,c} = 7$, magenta), was similar to without RR (9.5 ± 2.5%, UB = 3.9 ± 0.9%, $n^{s,c} = 9$, blue) (mean ± SEM, p = 0.31). Removal of the outlier in the RR group did not change this outcome. **D:** n^{n}(magenta) = 146, n^{n}(blue) = 188. **E:** The efficacy in a single disconnected culture with additional GsMTx-4 (10.1 ± 2.9%, UB = 2.1 ± 0.3%, $n^{s} = 5$, orange), was similar to without GsMTx-4 (11.4 ± 6.1%, UB = 2.7 ± 0.4%, $n^{s} = 5$, blue) (mean ± SEM, p = 0.43). **F:** n^{n}(orange) = 278, n^{n}(blue) = 220. (For interpretation of the references to colour in this figure legend, the reader is referred to the Web version of this article.)

didn't significantly affect the efficacy of US. This considerably narrows down the list of candidate channels.

This result conflicts with a recent study reporting that TRPA1 disruption *did* eliminate the response in hippocampal neurons [20]. However, as the authors suggest, they probably actually blocked the response in astrocytes, and measured the downstream effect on the neurons. This is an example of the complexity in interpreting observations from connected networks.

GsMTx-4, a blocker of Piezo1 and TRPC(1,5,6) channels [71–73], was applied to a single culture (Fig. 5E). As with RR, GsMTx-4 didn't significantly reduce the efficacy of US.

This conflicts with a recent study showing GsMTx-4 *did* eliminate the response in cortical cultures [23]. One possible cause of this discrepancy may be that certain MS channels, that are not blocked by GsMTx-4, and are much more highly expressed in the hippocampus than in the cortex (such as TRPM3 [74]), may be able to support a response in the hippocampal cultures, even when the other GsMTx-4 sensitive channels are blocked, but are not able to support a response in the cortex, due to their low level of expression there. Additionally, we used GsMTx-4 at a moderate concentration of twice the IC_{50} (in reference to TRPC channels), while they used a much higher concentration (1 μM vs 40 μM), which may have increased blocking efficacy or may block a broader array of channels.

The response is shown in Fig. 5D,F. The responses from cultures with RR had a higher amplitude (0.5 ± 0.06 ΔF/F, n^{n} = 146 vs. 0.2 ± 0.02 ΔF/F, n^{n} = 188; $p < 0.001$) and a longer duration (1.12 ± 0.08 vs. 0.85 ± 0.04 s, $p < 0.01$) than from cultures without RR (mean ± SEM). The responses from the culture with GsMTx-4 also had a higher amplitude (0.42 ± 0.05 ΔF/F, n^{n} = 278 vs. 0.23 ± 0.01 ΔF/F, n^{n} = 220; $p < 0.001$), and a longer duration (1.1 ± 0.05 vs. 0.76 ± 0.03 s, $p < 0.001$) than the responses from the

culture without GsMTx-4 (mean ± SEM). A possible cause for this is the inhibitory effect these compounds can have on large-conductance calcium-activated potassium channels [75,76], which contribute to post-AP repolarization [77].

These results do not rule out the possible relevance of other MS channels or receptors. On the contrary, we believe this remains the most probable mechanism generating the effects we observe.

3.8. Attrition effects were dominant and occurred at the single-cell level

In disconnected cultures, after an initial successful stimulation at a given pressure, the following stimulations were not effective until the pressure was increased, at which point another successful stimulation would occur. This could be repeated for several stimulations (example in Supplementary Fig. S8). In order to avoid these attrition related confounds, in most of the experiments described only the first stimulation was used.

Fig. 6A compares the first stimulation and the following three at the same pressure (with a 25 min recovery period between stimulations). While the first stimulation was effective, the following three were much less effective. These three following stimulations didn't differ in their efficacy (Supplementary Fig. S9).

To check if an even longer recovery time made repeated stimulations more effective, we increased the time between consecutive stimulations to 3 days. In order to do this, we used GCaMP, a genetically encoded calcium indicator that doesn't significantly reduce the viability of the cultures, and thus the cultures can be imaged over an extended period. Connected cultures were stimulated several times, and then returned to the incubator. After three days, the cultures were first checked for spontaneous activity to ensure their viability, then pharmacologically disconnected, and stimulated again. Fig. 6C shows the response (after the 3-day recovery period) in these previously stimulated cultures, and for reference the response in fresh disconnected cultures that were not previously stimulated. We can see that even after this 3-day recovery period, attrition effects remained, and there was no observable response in the previously stimulated cultures.

Increases in pressure did generate additional successful stimulations, with no need for an extended recovery time. We examined if this resulted from new cells being recruited at higher intensities, or if the same cells that were responsive to the first stimulation but didn't respond to additional stimulations at the same pressure, became responsive again at higher pressures.

Indeed, most of the cells that were responsive to a first, lower-pressure (0.35 MPa) stimulation, were also responsive to a following, higher-pressure (0.67 MPa) stimulation (78.8 ± 4.6%, mean ± SEM, $n^{s,c} = 8$). However, most of the cells that were responsive to a following higher pressure stimulation were new cells that didn't previously respond to a lower pressure stimulation (74.3 ± 6.7%, mean ± SEM, $n^{s,c} = 8$). Fig. 6D shows an example. This indicates that the attrition effects occur, at least partially, at the single-cell level.

Fig. 6E compares the response to the lower-pressure stimulation in cells that responded only to the lower-pressure stimulation, and in cells that also responded to a later higher-pressure stimulation. There was no difference, and thus no indication of different processes taking place during the first stimulation.

These observations align with several studies showing that repeated or continued US stimulation coincides with a degradation in the response [44,78–80]. They may also be related to reports of US having long-term effects in-vivo, at timescales ranging from minutes [16,80–84] to weeks [85,86]. The mechanism responsible for attrition is unclear. One possibility is that MS channels undergo inactivation after being affected by US, and that other MS channels with higher stimulation thresholds are activated by the following higher-pressure pulse. MS channels may also undergo adaptation, requiring higher pressures to reactivate [87]. Another possibility is that the adherence of the cells to the glass is partially disrupted, reducing associated US shear forces, requiring an increase in US pressure for subsequent stimulation.

The ability of cells to respond multiple times to stimulation indicates that their viability is not dramatically disrupted by stimulation. This is also supported by the calcium levels in the responsive cells returning to baseline fairly quickly after stimulation.

3.9. Experimental limitations

One potential issue is our use of a glass substrate. Its rigidity may affect the mechanical sensitivities of the neurons grown on it [88]. Neurons in flat cultures also grow and connect differently than neurons in the complex 3D environment of the brain. Additionally, the glass-neuron interface may subject neurons to unphysiological shear forces under US [89].

A second potential issue is that our experiments were conducted at room temperature, which may alter the dynamics of cellular processes in comparison to physiological temperatures [90,91]. Additionally, our calcium concentration was modified from that of other in-vitro studies, to better represent the concentration in-vivo [92]. This may complicate comparing results, as calcium concentrations can substantially affect excitability in these cultures [93].

Third, mechanisms which we found to be negligible in our experimental conditions, may still be relevant at different stimulation parameters, or when targeting different neuronal populations. Additionally, our pharmacologically disconnected cultured neurons are not fully representative of neurons in vivo, and thus our conclusions may not completely translate to that domain.

A very recent publication by Yoo et al. (2022) [94] examined US stimulation of cortical neurons cultured on a flexible substrate. Their results complement and support our conclusions that poration, heating, and NBLS effects are not involved. Furthermore, their results using pharmacological interventions with RR and suramin align with ours, despite methodological differences. Their study provides substantial evidence implicating MS channels in the mechanism.

4. Conclusion

In conclusion, our results detract from mechanistic theories that implicate cavitation, heating, non-transient membrane pores >1.5 nm, pre-synaptic release, or gradual effects. They implicate a post-synaptic mechanism upstream of the AP process and narrow down the list of relevant receptors and ion channels.

We hope this work will advance US neurostimulation and help realize its potential as an effective tool for research and the treatment of human distress.

Funding

This work was supported by the Israel Science Foundation [grant #2767/20] and the MINERVA Stiftung with funds from the BMBF of the Federal Republic of Germany. Funding sources had no involvement in the study itself.

Data availability

Data will be made available upon reasonable request.

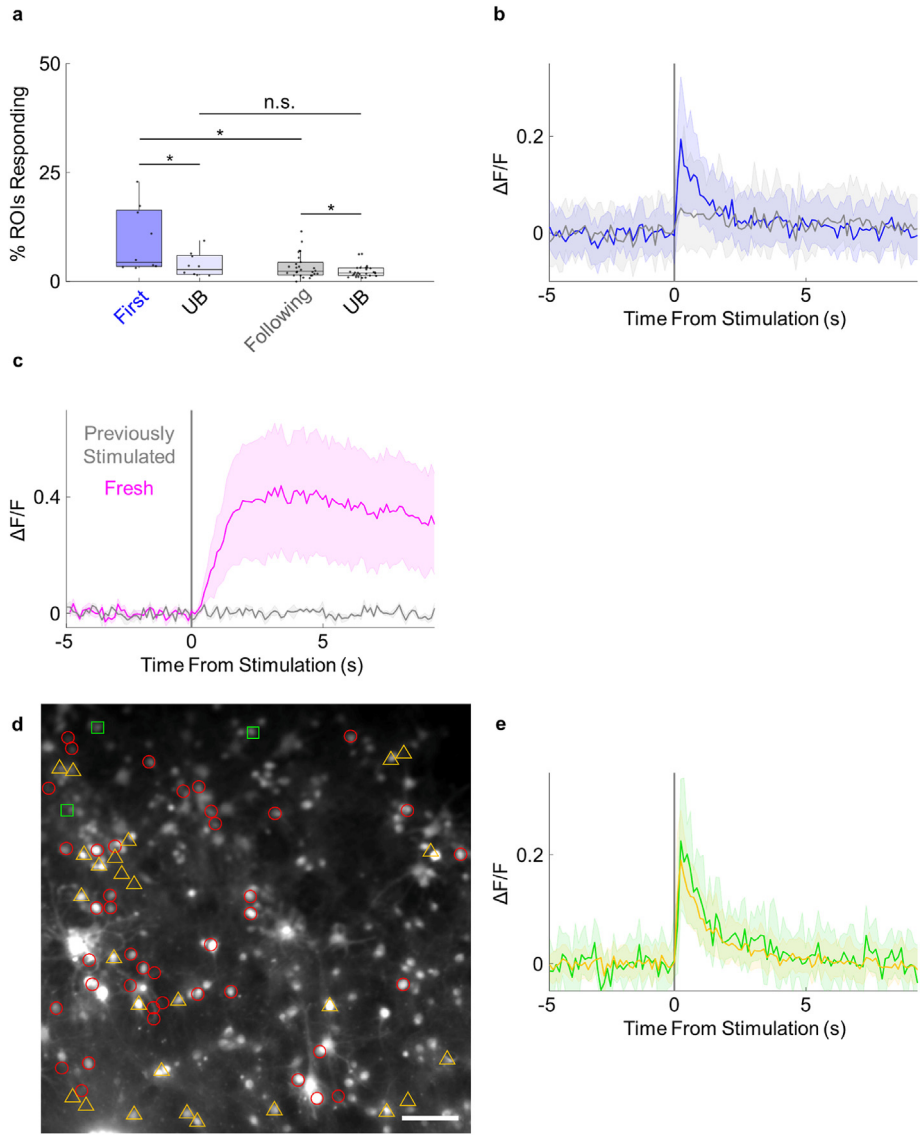

Fig. 6. Response attrition
A: Percentage of generally active cells responsive to stimulations at a constant pressure with a 25 min recovery time between pulses, in disconnected cultures. After an initial successful stimulation at the given pressure (9.5 ± 2.5%, UB = 3.9 ± 0.9%, $n^{s,c} = 9$, blue), the following 3 stimulations at the same pressure had a low efficacy, close to their unstimulated baseline activity (3.4 ± 0.5%, UB = 2.3 ± 0.3%, $n^{s} = 27$, gray) (mean ± SEM). UB - unstimulated baseline activity. **B:** Median calcium traces from responsive cells, corresponding to **A**. n^{n}(blue) = 188, n^{n}(gray) = 225. **C:** Response to stimulation in disconnected cultures that were previously stimulated at the same pressure 3 days before (gray, $n^{s,c} = 3$), and in fresh disconnected cultures that were not previously stimulated (magenta, $n^{s,c} = 6$). Shown is the mean calcium trace from the full FOV. SEM shown shaded. Calcium imaging was done using GCaMP. **D, E:** Successful stimulation with a lower-pressure pulse, followed by a second successful stimulation with a higher-pressure pulse, in disconnected cultures. **D:** An example culture. Shown are cells responsive only to the first stimulation at the lower pressure (green squares), those responsive only to the following stimulation at the higher pressure, (red circles), and those responsive to both stimulations (orange triangles). 90% (26 of 29) of the cells responsive to the first stimulation were also responsive to the second stimulation in this example. Scale bar: 100 μm. **E:** Median calcium traces of the response to the lower-pressure stimulation, in the cells that responded only to the lower-pressure stimulation (green, $n^{n} = 30$), and in those that responded to both pressures (orange, $n^{n} = 124$)($n^{c} = 8$). (For interpretation of the references to colour in this figure legend, the reader is referred to the Web version of this article.)

Declarations of interest

None.

CRediT authorship contribution statement

Eyal Weinreb: Conceptualization, Methodology, Writing, Investigation, Software, Analysis, Visualization. **Elisha Moses:** Conceptualization, Methodology, Writing, Administration, Supervision, Funding, Resources.

Acknowledgments

We would like to thank Victor Steinberg and Daniella Goldfarb for advice and equipment, Menachem Segal for fruitful discussions, Rony Paz for guidance, Dominik Freche for assistance with model implementation, and Inbar Zohar for assistance with experiments.

Appendix A Supplementary

The supplementary to this article can be found online at https://doi.org/10.1016/j.brs.2022.05.004.

References

[1] Blackmore J, Shrivastava S, Sallet J, Butler CR, Cleveland RO. Ultrasound neuromodulation: a review of results, mechanisms and safety. Ultrasound Med Biol 2019;45:1509–36. https://doi.org/10.1016/j.ultrasmedbio.2018.12.015.

[2] Darrow DP. Focused ultrasound for neuromodulation. Neurotherapeutics 2019;16:88–99. https://doi.org/10.1007/s13311-018-00691-3.

[3] Kubanek J. Neuromodulation with transcranial focused ultrasound. Neurosurg Focus 2018;44:1–6. https://doi.org/10.3171/2017.11.FOCUS17621.

[4] Naor O, Krupa S, Shoham S. Ultrasonic neuromodulation. J Neural Eng 2016;13:031003. https://doi.org/10.1088/1741-2560/13/3/031003.

[5] Velling VA, Shklyaruk SP. Modulation of the functional state of the brain with the aid of focused ultrasonic action. Neurosci Behav Physiol 1988;18:369–75. https://doi.org/10.1007/BF01193880.

[6] Plaksin M, Shoham S, Kimmel E. Intramembrane cavitation as a predictive bio-piezoelectric mechanism for ultrasonic brain stimulation. Phys Rev X 2014;4:011004. https://doi.org/10.1103/PhysRevX.4.011004.

[7] Shapiro MG, Homma K, Villarreal S, Richter C, Bezanilla F. Infrared light excites cells by changing their electrical capacitance. Nat Commun 2012;3:736. https://doi.org/10.1038/ncomms1742.

[8] Constans C, Mateo P, Tanter M, Aubry JF. Potential impact of thermal effects during ultrasonic neurostimulation: retrospective numerical estimation of temperature elevation in seven rodent setups. Phys Med Biol 2018;63. https://doi.org/10.1088/1361-6560/aaa15c.

[9] Darrow DP, O'Brien P, Richner TJ, Netoff TI, Ebbini ES. Reversible neuroinhibition by focused ultrasound is mediated by a thermal mechanism. Brain Stimul 2019;12:1439–47. https://doi.org/10.1016/j.brs.2019.07.015.

[10] Sharabi S, Daniels D, Last D, Guez D, Zivli Z, Castel D, et al. Non-thermal focused ultrasound induced reversible reduction of essential tremor in a rat model. Brain Stimul 2019;12:1–8. https://doi.org/10.1016/j.brs.2018.08.014.

[11] Spivak NM, Schafer ME, Bystritsky A. Reversible neuroinhibition does not require a thermal mechanism. Brain Stimul 2019;13:262. https://doi.org/10.1016/j.brs.2019.09.007.

[12] Darrow DP, O'Brien P, Richner T, Netoff TI, Ebbini ES. A thermal mechanism underlies tFUS neuromodulation. Brain Stimul 2019;13:327–8. https://doi.org/10.1016/j.brs.2019.10.018.

[13] Tufail Y, Matyushov A, Baldwin N, Tauchmann ML, Georges J, Yoshihiro A, et al. Transcranial pulsed ultrasound stimulates intact brain circuits. Neuron 2010;66:681–94. https://doi.org/10.1016/j.neuron.2010.05.008.

[14] Khraiche ML, Phillips WB, Jackson N, Muthuswamy J. Ultrasound induced increase in excitability of single neurons. IEEE Eng. Med. Biol. 2008;2008:4246–9. https://doi.org/10.1109/IEMBS.2008.4650147.

[15] Lee W, Kim H-C, Jung Y, Chung YA, Song I-U, Lee J-H, et al. Transcranial focused ultrasound stimulation of human primary visual cortex. Sci Rep 2016;6:34026. https://doi.org/10.1038/srep34026.

[16] Yoo S-S, Bystritsky A, Lee J-H, Zhang Y, Fischer K, Min B-K, et al. Focused ultrasound modulates region-specific brain activity. Neuroimage 2011;56:1267–75. https://doi.org/10.1016/j.neuroimage.2011.02.058.

[17] Tyler WJ, Tufail Y, Finsterwald M, Tauchmann ML, Olson EJ, Majestic C. Remote excitation of neuronal circuits using low-intensity, low-frequency ultrasound. PLoS One 2008;3:e3511. https://doi.org/10.1371/journal.pone.0003511.

[18] Prieto ML, Oralkan Ö, Khuri-Yakub BT, Maduke M. Dynamic response of model lipid membranes to ultrasonic radiation force. PLoS One 2013;8:e77115. https://doi.org/10.1371/journal.pone.0077115.

[19] Mihran RT, Barnes FS, Wachtel H. Temporally-specific modification of myelinated axon excitability in vitro following a single ultrasound pulse. Ultrasound Med Biol 1990;16:297–309. https://doi.org/10.1016/0301-5629(90)90008-Z.

[20] Oh S-J, Lee JM, Kim H-B, Lee J, Han S, Bae JY, et al. Ultrasonic neuromodulation via astrocytic TRPA1. Curr Biol 2019;29:3386–401. https://doi.org/10.1016/j.cub.2019.08.021. e8.

[21] Prieto ML, Firouzi K, Khuri-Yakub BT, Maduke M. Activation of Piezo1 but not NaV1.2 channels by ultrasound at 43 MHz. Ultrasound Med Biol 2018;44:1217–32. https://doi.org/10.1016/j.ultrasmedbio.2017.12.020.

[22] Sorum B, Rietmeijer RA, Gopakumar K, Adesnik H, Brohawn SG. Ultrasound activates mechanosensitive TRAAK K + channels through the lipid membrane. Proc Natl Acad Sci Unit States Am 2021;118:e2006980118. https://doi.org/10.1073/pnas.2006980118.

[23] Qiu Z, Guo J, Kala S, Zhu J, Xian Q, Qiu W, et al. The mechanosensitive ion channel Piezo1 significantly mediates in vitro ultrasonic stimulation of neurons. iScience 2019;21:448–57. https://doi.org/10.1016/j.isci.2019.10.037.

[24] Kubanek J, Shi J, Marsh J, Chen D, Deng C, Cui J. Ultrasound modulates ion channel currents. Sci Rep 2016;6:1–14. https://doi.org/10.1038/srep24170.

[25] Menz MD, Ye P, Firouzi K, Nikoozadeh A, Pauly KB, Khuri-Yakub P, et al. Radiation force as a physical mechanism for ultrasonic neurostimulation of the ex vivo retina. J Neurosci 2019;39:6251–64. https://doi.org/10.1523/jneurosci.2394-18.2019.

[26] Constans C, Deffieux T, Pouget P, Tanter M, Aubry JF. A 200-1380-kHz quadrifrequency focused ultrasound transducer for neurostimulation in rodents and primates: transcranial in vitro calibration and numerical study of the influence of skull cavity. IEEE Trans Ultrason Ferroelectrics Freq Control 2017;64:717–24. https://doi.org/10.1109/TUFFC.2017.2651648.

[27] Hensel K, Mienkina MP, Schmitz G. Analysis of ultrasound fields in cell culture wells for in vitro ultrasound therapy experiments. Ultrasound Med Biol 2011;37:2105–15. https://doi.org/10.1016/j.ultrasmedbio.2011.09.007.

[28] O'Reilly MA, Huang Y, Hynynen K. The impact of standing wave effects on transcranial focused ultrasound disruption of the blood–brain barrier in a rat model. Phys Med Biol 2010;55:5251–67. https://doi.org/10.1088/0031-9155/55/18/001.

[29] Deffieux T, Konofagou EE. Numerical study of a simple transcranial focused ultrasound system applied to blood-brain barrier opening. IEEE Trans Ultrason Ferroelectrics Freq Control 2010;57:2637–53. https://doi.org/10.1109/TUFFC.2010.1738.

[30] Younan Y, Deffieux T, Larrat B, Fink M, Tanter M, Aubry J-F. Influence of the pressure field distribution in transcranial ultrasonic neurostimulation. Med Phys 2013;40:082902. https://doi.org/10.1118/1.4812423.

[31] Wattiez N, Constans C, Deffieux T, Daye PM, Tanter M, Aubry JF, et al. Transcranial ultrasonic stimulation modulates single-neuron discharge in macaques performing an antisaccade task. Brain Stimul 2017;10:1024–31. https://doi.org/10.1016/j.brs.2017.07.007.

[32] Mueller JK, Ai L, Bansal P, Legon W. Numerical evaluation of the skull for human neuromodulation with transcranial focused ultrasound. J Neural Eng 2017;14:066012. https://doi.org/10.1088/1741-2552/aa843e.

[33] Folloni D, Verhagen L, Mars RB, Fouragnan E, Constans C, Aubry JF, et al. Manipulation of subcortical and deep cortical activity in the primate brain using transcranial focused ultrasound stimulation. Neuron 2019;101:1109–16. https://doi.org/10.1016/j.neuron.2019.01.019. e5.

[34] Mohammadjavadi M, Ye PP, Xia A, Brown J, Popelka G, Pauly KB. Elimination of peripheral auditory pathway activation does not affect motor responses from ultrasound neuromodulation. Brain Stimul 2019;12:901–10. https://doi.org/10.1016/j.brs.2019.03.005.

[35] Segal M, Manor D. Confocal microscopic imaging of [Ca2+]i in cultured rat hippocampal neurons following exposure to N-methyl-D-aspartate. J Physiol 1992;448:655–76. https://doi.org/10.1113/jphysiol.1992.sp019063.

[36] Papa M, Bundman M, Greenberger V, Segal M. Morphological analysis of dendritic spine development in primary cultures of hippocampal neurons. J Neurosci 1995;15:1–11. https://doi.org/10.1523/JNEUROSCI.15-01-00001.1995.

[37] Soriano J, Martínez MR, Tlusty T, Moses E. Development of input connections in neural cultures. Proc Natl Acad Sci Unit States Am 2008;105:13758–63. https://doi.org/10.1073/pnas.0707492105.

[38] Eckmann JP, Feinerman O, Gruendlinger L, Moses E, Soriano J, Tlusty T. The physics of living neural networks. Phys Rep 2007;449:54–76. https://doi.org/10.1016/j.physrep.2007.02.014.

[39] Gateau J, Aubry J-F, Chauvet D, Boch A-L, Fink M, Tanter M. In vivo bubble nucleation probability in sheep brain tissue. Phys Med Biol 2011;56:7001–15. https://doi.org/10.1088/0031-9155/56/22/001.

[40] McLaughlan J, Rivens I, Leighton T, ter Haar G. A study of bubble activity generated in ex vivo tissue by high intensity focused ultrasound. Ultrasound Med Biol 2010;36:1327–44. https://doi.org/10.1016/j.ultrasmedbio.2010.05.011.

[41] Manuel TJ, Kusunose J, Zhan X, Lv X, Kang E, Yang A, et al. Ultrasound neuromodulation depends on pulse repetition frequency and can modulate inhibitory effects of TTX. Sci Rep 2020;10:1–10. https://doi.org/10.1038/s41598-020-72189-y.

[42] Qi X, Lyu K, Meng L, Li C, Zhang H, Niu L, et al. Low-intensity ultrasound causes direct excitation of auditory cortical neurons. Neural Plast 2021;2021:1–10. https://doi.org/10.1155/2021/8855055.

[43] Suarez-Castellanos IM, Dossi E, Vion-Bailly J, Salette L, Chapelon J-Y, Carpentier A, et al. Spatio-temporal characterization of causal electrophysiological activity stimulated by single pulse focused ultrasound: an ex vivo study on hippocampal brain slices. J Neural Eng 2021;18:026022. https://doi.org/10.1088/1741-2552/abdfb1.

[44] Prieto ML, Firouzi K, Khuri-Yakub BT, Madison DV, Maduke M. Spike frequency-dependent inhibition and excitation of neural activity by high-frequency ultrasound. J Gen Physiol 2020;152. https://doi.org/10.1085/jgp.202012672.

[45] Han H, Hwang SY, Akram F, Jeon HJ, Nam SB, Jun SB, et al. Neural activity modulation via ultrasound stimulation measured on multi-channel electrodes. In: World congr. Eng., I. London, U.K.: International Association of Engineers; 2014. p. 5–8. Available from: http://www.iaeng.org/publication/WCE2014/WCE2014_pp604-607.pdf.

[46] Muratore R, LaManna J, Szulman E, Kalisz A, Lamprecht M, Simon M, et al. Bioeffective ultrasound at very low doses: reversible manipulation of neuronal cell morphology and function in vitro. AIP Conf Proc 2009;113:25–9. https://doi.org/10.1063/1.3131426.

[47] Bachtold MR, Rinaldi PC, Jones JP, Reines F, Price LR. Focused ultrasound modifications of neural circuit activity in a mammalian brain. Ultrasound Med Biol 1998;24:557–65. https://doi.org/10.1016/S0301-5629(98)00014-3.

[48] Menz MD, Oralkan O, Khuri-Yakub PT, Baccus SA. Precise neural stimulation in the retina using focused ultrasound. J Neurosci 2013;33:4550–60. https://doi.org/10.1523/JNEUROSCI.3521-12.2013.

[49] Jiang Q, Li G, Zhao H, Sheng W, Yue L, Su M, et al. Temporal neuromodulation of retinal ganglion cells by low-frequency focused ultrasound stimulation. IEEE Trans Neural Syst Rehabil Eng 2018;26:969–76. https://doi.org/10.1109/TNSRE.2018.2821194.

[50] Kim HB, Swanberg KM, Han HS, Kim JC, Kim JW, Lee S, et al. Prolonged stimulation with low-intensity ultrasound induces delayed increases in spontaneous hippocampal culture spiking activity. J Neurosci Res 2017;95:885–96. https://doi.org/10.1002/jnr.23845.
[51] Breskin I, Soriano J, Moses E, Tlusty T. Percolation in living neural networks. Phys Rev Lett 2006;97:188102. https://doi.org/10.1103/PhysRevLett.97.188102.
[52] Han S, Kim M, Kim H, Shin H, Youn I. Ketamine inhibits ultrasound stimulation-induced neuromodulation by blocking cortical neuron activity. Ultrasound Med Biol 2018;44:635–46. https://doi.org/10.1016/j.ultrasmedbio.2017.11.008.
[53] Stern S, Agudelo-Toro A, Rotem A, Moses E, Neef A. Chronaxie measurements in patterned neuronal cultures from rat hippocampus. PLoS One 2015;10:e0132577. https://doi.org/10.1371/journal.pone.0132577.
[54] Kougioumoutzakis A, Pelletier JG, Laplante I, Khlaifia A, Lacaille J-C. TRPC1 mediates slow excitatory synaptic transmission in hippocampal oriens/alveus interneurons. Mol Brain 2020;13:12. https://doi.org/10.1186/s13041-020-0558-9.
[55] Zhang Y, Abiraman K, Li H, Pierce DM, Tzingounis AV, Lykotrafitis G. Modeling of the axon membrane skeleton structure and implications for its mechanical properties. PLoS Comput Biol 2017;13:e1005407. https://doi.org/10.1371/journal.pcbi.1005407.
[56] Bowman AM, Nesin OM, Pakhomova ON, Pakhomov AG. Analysis of plasma membrane integrity by fluorescent detection of Tl(+) uptake. J Membr Biol 2010;236:15–26. https://doi.org/10.1007/s00232-010-9269-y.
[57] Pakhomov AG, Bowman AM, Ibey BL, Andre FM, Pakhomova ON, Schoenbach KH. Lipid nanopores can form a stable, ion channel-like conduction pathway in cell membrane. Biochem Biophys Res Commun 2009;385:181–6. https://doi.org/10.1016/j.bbrc.2009.05.035.
[58] Ahmadi F, McLoughlin IV, Chauhan S, Ter-Haar G. Bio-effects and safety of low-intensity, low-frequency ultrasonic exposure. Prog Biophys Mol Biol 2012;108:119–38. https://doi.org/10.1016/j.pbiomolbio.2012.01.004.
[59] Vykhodtseva NI, Hynynen K, Damianou C. Histologic effects of high intensity pulsed ultrasound exposure with subharmonic emission in rabbit brain in vivo. Ultrasound Med Biol 1995;21:969–79. https://doi.org/10.1016/0301-5629(95)00038-S.
[60] F.D.A.. Information for manufacturers seeking marketing clearance of diagnostic ultrasound systems and transducers. MD: Silver Spring; 2008.
[61] Wei L, Mousawi F, Li D, Roger S, Li J, Yang X, et al. Adenosine triphosphate release and P2 receptor signaling in Piezo1 channel-dependent mechanoregulation. Front Pharmacol 2019;10:1–10. https://doi.org/10.3389/fphar.2019.01304.
[62] Gill JS, Hobday KL, Windebank AJ. Mechanism of suramin toxicity in stable myelinating dorsal root ganglion cultures. Exp Neurol 1995;133:113–24. https://doi.org/10.1006/exnr.1995.1014.
[63] Kamimura HAS, Wang S, Chen H, Wang Q, Aurup C, Acosta C, et al. Focused ultrasound neuromodulation of cortical and subcortical brain structures using 1.9 MHz. Med Phys 2016;43:5730–5. https://doi.org/10.1118/1.4963208.
[64] King RL, Brown JR, Newsome WT, Pauly KB. Effective parameters for ultrasound-induced in vivo neurostimulation. Ultrasound Med Biol 2013;39:312–31. https://doi.org/10.1016/j.ultrasmedbio.2012.09.009.
[65] Li G-F, Zhao H-X, Zhou H, Yan F, Wang J-Y, Xu C-X, et al. Improved anatomical specificity of non-invasive neuro-stimulation by high frequency (5 MHz) ultrasound. Sci Rep 2016;6:1–11. https://doi.org/10.1038/srep24738.
[66] Burks SR, Lorsung RM, Nagle ME, Tu T-W, Frank JA. Focused ultrasound activates voltage-gated calcium channels through depolarizing TRPC1 sodium currents in kidney and skeletal muscle. Theranostics 2019;9:5517–31. https://doi.org/10.7150/thno.33876.
[67] Rountree CM, Meng C, Troy JB, Saggere L. Mechanical stimulation of the retina: therapeutic feasibility and cellular mechanism. IEEE Trans Neural Syst Rehabil Eng 2018;26:1075–83. https://doi.org/10.1109/TNSRE.2018.2822322.
[68] Clapham DE. SnapShot: mammalian TRP channels. Cell 2007;129. https://doi.org/10.1016/j.cell.2007.03.034. 220.e1-220.e2.
[69] Coste B, Mathur J, Schmidt M, Earley TJ, Ranade S, Petrus MJ, et al. Piezo1 and Piezo2 are essential components of distinct mechanically activated cation channels. Science 2010;330:55–60. https://doi.org/10.1126/science.1193270.
[70] Braun G, Lengyel M, Enyedi P, Czirják G. Differential sensitivity of TREK-1, TREK-2 and TRAAK background potassium channels to the polycationic dye ruthenium red. Br J Pharmacol 2015;172:1728–38. https://doi.org/10.1111/bph.13019.
[71] Bae C, Sachs F, Gottlieb PA. The mechanosensitive ion channel Piezo1 is inhibited by the peptide GsMTx-4. Biochemistry 2011;50:6295–300. https://doi.org/10.1021/bi200770q.
[72] Bowman CL, Gottlieb PA, Suchyna TM, Murphy YK, Sachs F. Mechanosensitive ion channels and the peptide inhibitor GsMTx-4: history, properties, mechanisms and pharmacology. Toxicon 2007;49:249–70. https://doi.org/10.1016/j.toxicon.2006.09.030.
[73] Gomis A, Soriano S, Belmonte C, Viana F. Hypoosmotic- and pressure-induced membrane stretch activate TRPC5 channels. J Physiol 2008;586:5633–49. https://doi.org/10.1113/jphysiol.2008.161257.
[74] Lein ES, Hawrylycz MJ, Ao N, Ayres M, Bensinger A, Bernard A, et al. Genome-wide atlas of gene expression in the adult mouse brain. Nature 2007;445:168–76. https://doi.org/10.1038/nature05453.
[75] Wu S-N, Jan C-R, Li H-F. Ruthenium red-mediated inhibition of large-conductance Ca2+-activated K+ channels in rat pituitary GH3 cells. J Pharmacol Exp Therapeut 1999;290:998–1005. Available from: https://jpet.aspetjournals.org/content/290/3/998.long.
[76] Li H, Xu J, Shen ZS, Wang GM, Tang M, Du XR, et al. The neuropeptide GsMTx4 inhibits a mechanosensitive BK channel through the voltage-dependent modification specific to mechano-gating. J Biol Chem 2019;294:11892–909. https://doi.org/10.1074/jbc.RA118.005511.
[77] Berkefeld H, Fakler B, Schulte U. Ca2+-activated K+ channels: from protein complexes to function. Physiol Rev 2010;90:1437–59. https://doi.org/10.1152/physrev.00049.2009.
[78] Kubanek J, Brown J, Ye P, Pauly KB, Moore T, Newsome W. Remote, brain region-specific control of choice behavior with ultrasonic waves. Sci Adv 2020;6:eaaz4193. https://doi.org/10.1126/sciadv.aaz4193.
[79] Takagi SF, Higashino S, Shibuya T, Osawa N. The actions of ultrasound on the myelinated nerve, the spinal cord and the brain. Jpn J Physiol 1960;10:183–93. https://doi.org/10.2170/jjphysiol.10.183.
[80] Hu JH, Ulrich WD. Effects of low-intensity ultrasound on the central nervous system of primates. Aviat Space Environ Med 1976;47:640–3.
[81] Dallapiazza RF, Timbie KF, Holmberg S, Gatesman J, Lopes MB, Price RJ, et al. Noninvasive neuromodulation and thalamic mapping with low-intensity focused ultrasound. J Neurosurg 2018;128:875–84. https://doi.org/10.3171/2016.11.JNS16976.
[82] Yoo SS, Yoon K, Croce P, Cammalleri A, Margolin RW, Lee W. Focused ultrasound brain stimulation to anesthetized rats induces long-term changes in somatosensory evoked potentials. Int J Imag Syst Technol 2018;28:106–12. https://doi.org/10.1002/ima.22262.
[83] Verhagen L, Gallea C, Folloni D, Constans C, Jensen DEA, Ahnine H, et al. Offline impact of transcranial focused ultrasound on cortical activation in primates. Elife 2019;8:1–28. https://doi.org/10.7554/eLife.40541.
[84] Pouget P, Frey S, Ahnine H, Attali D, Claron J, Constans C, et al. Neuronavigated repetitive transcranial ultrasound stimulation induces long-lasting and reversible effects on oculomotor performance in non-human primates. Front Physiol 2020;11:1042. https://doi.org/10.3389/fphys.2020.01042.
[85] Baek H, Pahk KJ, Kim MJ, Youn I, Kim H. Modulation of cerebellar cortical plasticity using low-intensity focused ultrasound for poststroke sensorimotor function recovery. Neurorehabilitation Neural Repair 2018;32:777–87. https://doi.org/10.1177/1545968318790022.
[86] Daniels D, Sharabi S, Last D, Guez D, Salomon S, Zivli Z, et al. Focused ultrasound-induced suppression of auditory evoked potentials in vivo. Ultrasound Med Biol 2018;44:1022–30. https://doi.org/10.1016/j.ultrasmedbio.2018.01.010.
[87] Wu J, Lewis AH, Grandl J. Touch, tension, and transduction – the function and regulation of piezo ion channels. Trends Biochem Sci 2017;42:57–71. https://doi.org/10.1016/j.tibs.2016.09.004.
[88] Pathak MM, Nourse JL, Tran T, Hwe J, Arulmoli J, Le DTT, et al. Stretch-activated ion channel Piezo1 directs lineage choice in human neural stem cells. Proc Natl Acad Sci Unit States Am 2014;111:16148–53. https://doi.org/10.1073/pnas.1409802111.
[89] Wu J. Acoustic streaming and its applications. Fluid 2018;3:108. https://doi.org/10.3390/fluids3040108.
[90] Reichlin S. Transient receptor potential (TRP) channels. In: Flockerzi V, Nilius B, editors. Handb. Exp. Pharmacol., 179. Berlin, Heidelberg: Springer Berlin Heidelberg; 2007. p. 366. https://doi.org/10.1007/978-3-540-34891-7.
[91] Maingret F, Lauritzen I, Patel AJ, Heurteaux C, Reyes R, Lesage F, et al. TREK-1 is a heat-activated background K+ channel. EMBO J 2000;19:2483–91. https://doi.org/10.1093/emboj/19.11.2483.
[92] Jones HC, Keep RF. Brain fluid calcium concentration and response to acute hypercalcaemia during development in the rat. J Physiol 1988;402:579–93. https://doi.org/10.1113/jphysiol.1988.sp017223.
[93] Penn Y, Segal M, Moses E. Network synchronization in hippocampal neurons. Proc Natl Acad Sci Unit States Am 2016;113:3341–6. https://doi.org/10.1073/pnas.1515105113.
[94] Yoo S, Mittelstein DR, Hurt RC, Lacroix J, Shapiro MG. Focused ultrasound excites cortical neurons via mechanosensitive calcium accumulation and ion channel amplification. Nat Commun 2022;13:493. https://doi.org/10.1038/s41467-022-28040-1.